EC Journals.ASM.org

Role of Pex11p in Lipid Homeostasis in *Yarrowia lipolytica*

Rémi Dulermo,[a,b] Thierry Dulermo,[a,b] Heber Gamboa-Meléndez,[b] France Thevenieau,[c] Jean-Marc Nicaud[a,b]

INRA, UMR1319 Micalis, Jouy-en-Josas, France[a]; AgroParisTech, UMR Micalis, Jouy-en-Josas, France[b]; Sofiproteol, Direction Innovation, Paris, France[c]

Peroxisomes are essential organelles in the cells of most eukaryotes, from yeasts to mammals. Their role in β-oxidation is particularly essential in yeasts; for example, in *Saccharomyces cerevisiae*, fatty acid oxidation takes place solely in peroxisomes. In this species, peroxisome biogenesis occurs when lipids are present in the culture medium, and it involves the Pex11p protein family: ScPex11p, ScPex25p, ScPex27p, and ScPex34p. *Yarrowia lipolytica* has three Pex11p homologues, which are YALI0C04092p (YlPex11p), YALI0C04565p (YlPex11C), and YALI0D25498p (Pex11/25p). We found that these genes are regulated by oleic acid, and as has been observed in other organisms, *YlPEX11* deletion generated giant peroxisomes when mutant yeast were grown in oleic acid medium. Moreover, Δ*Ylpex11* was unable to grow on fatty acid medium and showed extreme dose-dependent sensitivity to oleic acid. Indeed, when the strain was grown in minimum medium with 0.5% glucose and 3% oleic acid, lipid body lysis and cell death were observed. Cell death and lipid body lysis may be partially explained by an imbalance in the expression of the genes involved in lipid storage, namely, *DGA1*, *DGA2*, and *LRO1*, as well as that of *TGL4*, which is involved in lipid remobilization. *TGL4* deletion and *DGA2* overexpression resulted in decreased oleic acid sensitivity and delayed cell death of Δ*Ylpex11*, which probably stemmed from the release of free fatty acids into the cytoplasm. All these results show that YlPex11p plays an important role in lipid homeostasis in *Y. lipolytica*.

Peroxisomes are organelles that play an important role in different cellular processes and particularly in β-oxidation. In yeasts, β-oxidation (the process that breaks down fatty acids) takes place solely in this organelle (1). Peroxisome biogenesis involves more than 30 proteins (Pex proteins), and most of them (e.g., Pex1p, Pex2p, etc.) are crucial for the uptake of matrix proteins (2). Certain other Pex proteins, such as Pex11p, are involved in peroxisome fission and proliferation in higher and lower eukaryotes (3–8).

In *Saccharomyces cerevisiae*, Pex11p (ScPex11p) is an inner membrane-associated homodimer protein, and it is one of the most abundant peroxisomal proteins resulting from oleic acid induction (3, 4, 9). In the absence of oleic acid, Δ*Scpex11* peroxisomes demonstrate a normal morphology, although they are larger and less abundant than peroxisomes found in the parental strain in the presence of oleic acid (3, 4, 10). Moreover, overexpression of *ScPEX11* increases the number of normal-sized peroxisomes, an observation that indicates that ScPex11p is involved in peroxisome elongation and fission (4). It has been shown that *PEX11*α and *PEX11*β of *Homo sapiens* and *PEX11c*, *PEX11d*, and *PEX11e* of *Arabidopsis thaliana* can complement the lack of ScPex11p function in Δ*Scpex11* mutants, which suggests that the role of Pex11p is conserved between *S. cerevisiae* and higher eukaryotes (8, 11).

The importance of Scpex11p remains unclear, as studies examining Δ*Scpex11* growth on fatty acid (FA) medium have yielded conflicting results. Indeed, Erdmann and Blobel (3) and Huber et al. (11) found that the strain did not grow on oleic acid. In contrast, Marshall et al. (4) and Rottensteiner et al. (12) found that Δ*Scpex11* was still able to grow but grew more slowly than the wild-type strain. Erdmann and Blobel (3) reported that Δ*Scpex11* still forms buds but that these buds lack peroxisomes, which suggests that growth on oleic acid is reduced because of differences in peroxisome inheritance. Moreover, it was shown that ScPex11p is involved in oxidation of medium-chain fatty acids (MCFA; C_8 or C_{12}) (10, 12). Authors have suggested that Pex11p is involved in transport of MCFA or cofactors needed to degrade MCFA (10).

ScPex11p is activated by the phosphorylation of S165 and S167 via a Pho85p kinase-dependent pathway. The absence of these specific phosphorylation sites produces the same effect as that seen in the Δ*Scpex11* mutant (13). However, Pex11p regulation differs in other organisms. In *Pichia pastoris*, for instance, PpPex11p is activated by the phosphorylation of S174 by the fission machinery protein Fis1p (14), which recruits proteins, such as Mdv1p, Caf4p, and Dnm1p, that are involved in mitochondrion and peroxisome division (15).

In *S. cerevisiae*, two other Pex11p family proteins, Pex25p and Pex27p, also participate in peroxisome proliferation. Cells lacking one of these proteins contain fewer and enlarged peroxisomes, similar to the Δ*Scpex11* phenotype (12, 16–18). Interestingly, in contrast to the respective single mutants, the Δ*Scpex11* Δ*Scpex25* Δ*Scpex27* triple mutant is unable to grow on oleic acid and has impaired peroxisomal protein import. This result suggests that members of the Pex11p family play a generalized role in peroxisome biogenesis, possibly assisting in protein uptake and thus facilitating growth on FA medium (12). A recent study showed that, although ScPex11p keeps peroxisomes metabolically active and promotes the proliferation of preexisting peroxisomes,

Received 19 March 2015 **Accepted** 25 March 2015

Accepted manuscript posted online 27 March 2015

Citation Dulermo R, Dulermo T, Gamboa-Meléndez H, Thevenieau F, Nicaud J-M. 2015. Role of Pex11p in lipid homeostasis in *Yarrowia lipolytica*. Eukaryot Cell 14:511–525. doi:10.1128/EC.00051-15.

Address correspondence to Jean-Marc Nicaud, jean-marc.nicaud@grignon.inra.fr.

Supplemental material for this article may be found at http://dx.doi.org/10.1128/EC.00051-15.

Copyright © 2015, American Society for Microbiology. All Rights Reserved.

doi:10.1128/EC.00051-15

TABLE 1 Strains and plasmids

Strain or plasmid	Genotype or other relevant characteristics	Source or reference
E. coli strain		
DH5α	ϕ80d*lacZ*ΔM15 *recA1 endA1 gyrA96 thi-1 hsdR17*(r_K^- m_K^+) *supE44 relA1 deoR* Δ*(lacZYA-argF)U169*	Promega
Y. lipolytica strains		
W29	*MAT***a**, wild type	21
Po1d	*MAT***a** *ura3-302 leu2-270 xpr2-322*	21
JMY330	Po1d (Ura^+ Leu^-)	22
JMY2900	Po1d (Ura^+ Leu^+)	F. Brunel, unpublished data
JMY2950	Po1d *Ylpex11*::*URA3ex* (Ura^+ Leu^-)	This study
JMY3165	JMY330 + p*TEF-RedStar2SKL-LEU2*ex (Ura^+ Leu^+)	This study
JMY3170	Po1d *Ylpex11*::*URA3*ex + p*TEF-RedStar2SKL-LEU2*ex (Ura^+ Leu^+)	This study
JMY3227	Po1d *Ylpex11*::*URA3*ex + *LEU2*ex (Ura^+ Leu^+)	This study
JMY3666	JMY2950 + p*TEF-YlPEX11-LEU2*ex (Ura^+ Leu^+)	This study
JMY3987	JMY2950 + *tgl4*::*LEU2ex* (Ura^+ Leu^+)	This study
JMY4037	JMY3987 (Ura^- Leu^-)	This study
JMY4072	JMY4037 + p*TEF-DGA2-LEU2ex* (Ura^- Leu^+)	This study
JMY4093	Y2950 + p*TEF-DGA2-LEU2ex* (Ura^+ Leu^+)	This study
JMY4729	Y2900 + p*TEF-POT1-GFP* (Ura^- Leu^+ Hyg^r)	This study
JMY4730	Y3227 + p*TEF-POT1-GFP* (Ura^- Leu^+ Hyg^r)	This study
Plasmids		
pCR4Blunt-TOPO	Cloning vector	Invitrogen
JMP803	JMP62-p*POX2-URA3*ex	22
JMP1132	JMP62-p*TEF-DGA2-URA3ex*	23
JMP1364	pCR4Blunt-TOPO + *TGL4* UpDn-*LEU2ex*	24
JMP1392	JMP62-p*TEF-RedStar2SKL-LEU2ex*	25
JMP1427	JMP62p*TEF-YFP-LEU2ex*	24
JMP1635	pCR4Blunt-TOPO + *YlPEX11* UpDn	This study
JMP1669	pCR4Blunt-TOPO + *YlPEX11* UpDn-*URA3*ex	This study
JMP1822	JMP62 p*TEF-DGA2-LEU2ex*	T. Rossignol, unpublished data
JMP1925	pCR4Blunt-TOPO + *YlPEX11*	This study
JMP2023	JMP62-pTEF- *YlPEX11-LEU2ex*	This study
JMP2616	JMP62 + p*TEF-YlPEX11-YFP-LEU2ex*	This study
JMP2652	pUB4 + p*TEF-POT1-GFP-Hyg*	26

ScPex25p is nonetheless needed to initiate membrane proliferation. Additionally, it seems that ScPex27p competes with ScPex25p, negatively affecting peroxisomal function (11). Recently, it was also found that another protein, ScPex34p, forms a homodimer and a heterodimer with ScPex11p, ScPex25p, and ScPex27p, and in fact, this protein appears to regulate peroxisome number in *S. cerevisiae* (17).

Yarrowia lipolytica is able to grow on different carbon sources, especially hydrophobic substrates such as oils, fatty acids, and alkanes (19). As peroxisomes play an essential role in FA oxidation in *S. cerevisiae* (2) and *P. pastoris* (20), we expect that Pex11p homologues may be essential for growth on fatty acids in *Y. lipolytica* and answer definitively questions about the fundamental role of *PEX11* in lipid metabolism in eukaryotes. *YALI0C04092*, *YALI0C04565*, and *YALI0D25498* all encode proteins containing a Pex11p domain. YALI0C04092p, the closest homologue of ScPex11p, was named YlPex11p, and its role in fatty acid oxidation and peroxisome fission is analyzed here. We found that *YALI0C04092* is essential for growth on FA medium and that its deletion results in enlarged peroxisomes in yeast grown in oleic acid medium. Surprisingly, the *YlPEX11* knockout yeast shows severely impaired, dose-dependent growth in FA accumulation medium (yeast nitrogen base [YNB] with 0.5% glucose and 3% oleic acid), and its lipid bodies lyse into the cytoplasm. This phenomenon may be due, in part, to an imbalance between the expression of genes involved in lipid storage, *DGA1*, *DGA2*, and *LRO1*, and the expression of the *TGL4* gene, which is involved in lipid remobilization. This imbalance probably increases free fatty acid (FFA) levels in the cytoplasm, leading to cell death, even if we cannot exclude the potential role of sphingolipids in this phenomenon.

MATERIALS AND METHODS

Yeast growth and culture conditions. The *Y. lipolytica* strains used in this study were derived from the wild-type *Y. lipolytica* W29 strain (ATCC 20460) (Table 1). The auxotrophic strain, PO1d (Leu^- Ura^-), has been described by Barth and Gaillardin (21). All the strains used in this study are listed in Table 1. Media and growth conditions for *Escherichia coli* have been previously described by Sambrook et al. (27), and those for *Y. lipolytica* have been described by Barth and Gaillardin (21). Rich medium (yeast extract-peptose-dextrose [YPD]) and minimal glucose medium (YNB) were prepared as previously described (28). The minimal medium (YNB) contained 0.17% (wt/vol) yeast nitrogen base (without amino acids and ammonium sulfate; YNBww; Difco, Paris, France), 0.5% (wt/vol) NH_4Cl, and 50 mM phosphate buffer (pH 6.8). As needed, this minimal medium was supplemented with uracil (0.1 g/liter) and/or leucine (0.1 g/liter). The $YNBD_{0.5}O_3$ medium contained 0.1% (wt/vol) yeast extract (Bacto-DB),

TABLE 2 List of primers

Primer	Sequence	Utilization
C04092UpNotI	GAATGCGGCCGCTAGCAGTTATGGAGATTGGC	Upstream fragment of *YlPEX11*
C04092UpIsceI	CGATTACCCTGTTATCCCTACCGGCGAGGCAAACGGACATC	
C04092DnNotI	GAATGCGGCCGCGAATCTGCTCCTCCTTAACG	Downstream fragment of *YlPEX11*
C04092DnIsceIIceuI	GGTAGGGATAACAGGGTAATCGTAACTATAACGGTCCTAAG GTAGCGATAGATAACTCGCAAGAGACG	
Ver1C04092	GACTGCATCTGGTCTAAGGG	Verification of *YlPEX11* disruption
Ver2C04092	ACCGCATACCTGCATCCTTG	
C04092Start	ATCAGGATCCACAATGTCCGTTTGCCTCGCCCAGAACCCC	Complementation/overexpression of *YlPEX11*
C04092End	CATCCTAGGCTAAGCAGTAGCGGCCCAGGCCTTCTGG	
C04092End2	CATCCTAGGGCAGTAGCGGCCCAGGCCTTCTGG	Complementation/overexpression of *YlPEX11-YFP*
TGL4-P1	TGATTGTTTCACCTGCCTCGACACC	Amplification of disruption cassette *tgl4*::*LEU2ex* using JMY2206 genomic DNA
TGL4-T2	CGAATGGAAGCTCCAAACAGCTTGACC	
TGL4-Ver1	TTAGATGAATGGTCCATAATCAGCC	Verification of *TGL4* disruption
TGL4-Ver2	CGTCGTCGAGGTAGATTCCCTT	
pTEF-start	GGGTATAAAAGACCACCGTCC	Verification of p*TEF-RedStar2SKL-LEU2*ex or p*TEF-YlPEX11-LEU2*ex insertion into the *Y. lipolytica* genome
61 stop	GTAGATAGTTGAGGTAGAAGTTG	
C04092F	GAGAAGGAGAAGGACACCA	*YlPEX11* expression by RT-PCR
C04092R	TTCTGGACACCCATAATACC	
C04565-F	GAGAAGAAGGCTGGAAAGAC	*YALI0C04565* expression by RT-PCR
C04565-R	CAGGTTGTCCACAATACCAC	
D25498-F	TGTCTCAGCAAAATTGGAGT	*YALI0D25498* expression by RT-PCR
D25498-R	TCGTTAGCGAGTTTGAACAG	
DGA1_F	TGTACCGATTCCAGCAGT	*DGA1* expression by RT-PCR
DGA1_R	GGTGTGGGAGATAAGGCAA	
DGA2_F	TTCTCATCTTCCAGTACGCCTA	*DGA2* expression by RT-PCR
DGA2_R	GGCAATAAGATTGAGACCGTT	
LRO1_F	CTCCGCCGACTTCTTTATG	*LRO1* expression by RT-PCR
LRO1_R	GAAGTATCCGTCTCGGTG	
TGL4-A1	GTTCGACAAGGAGCCTATT	*TGL4* expression by RT-PCR
TGL4-A2	GGTCAGATGCGGATGATAAAG	
ACT-A1	TCCAGGCCGTCCTCTCCC	*Actin* expression by RT-PCR
ACT-A2	GGCCAGCCATATCGAGTCGCA	

0.5% glucose, and 3% oleic acid. Solid media were obtained by adding 1.6% agar. To add the fatty acids to liquid or solid media, a 50:50 emulsion of fatty acids–10% pluronic acid was first prepared and heated at 80°C for 10 min before being added to the media. The following fatty acids were used in our study: $C_{6:0}$ (99%; Sigma-Aldrich), $C_{10:0}$ (99%; Sigma-Aldrich), $C_{14:0}$ (99%; Acros Organics), $C_{16:0}$ (99%; Sigma-Aldrich), and $C_{18:1}$ (70%; Sigma-Aldrich).

Plasmid construction. The deletion cassettes were largely generated by PCR amplification conducted in accordance with the procedure of Fickers and colleagues (29). First, the upstream (Up) and downstream (Dn) regions of a target gene were amplified using *Y. lipolytica* W29 genomic DNA as the template and the gene-specific Up and Dn oligonucleotides as primer pairs (Table 2). Primers UpISceI and DnIsceI contained an extension that allowed the introduction of the I-SceI restriction site, making it possible to construct an UpDn fragment via PCR fusion (see above).

To disrupt *YlPEX11*, primer pairs C04092UpNotI/C04092UpIsceI and C04092DnNotI/C04092DnIsceIIceuI were employed (Table 2). The Up and Dn regions were purified and used in a PCR fusion. The resulting UpDn fragment was ligated into pCR4Blunt-TOPO, yielding the JMP1635 construct. The *URA3ex* marker (from JMP803) was then introduced at the I-SceI site, yielding the JMP1669 construct containing the *Ylpex11*::*URA3ex* cassette. This plasmid was then digested with NotI to obtain the deletion cassette.

To disrupt *TGL4*, the primer pair TGL4-P1/TGL4-T2 was used (Table 2) to directly amplify the *tgl4*::*LEU2ex* cassette from JMY2206 genomic DNA (24).

The complementation cassette employed for the *Ylpex11*::*URA3ex* strain was created using the primer pair C04092Start/C04092End. *YlPEX11* was cloned into pCR4Blunt-TOPO and then digested with AvrII and BamHI and cloned into JMP1392 that had been previously digested by BamHI and AvrII; this generated JMP2023. The vector to localize

YlPex11p was constructed with primer pair C04092Start/C04092End2. After digestion by BamHI and AvrII, the PCR fragment was cloned into JMP1427, carrying yellow fluorescent protein (YFP), to give JMP2616. *YlPEX11* and *YlPEX11-YFP* were expressed under the constitutive and strong promoter p*TEF*. The resulting plasmids were then digested with NotI to release the complementation cassette.

To acquire the *DGA2* overexpression cassette, JMP1132 was digested with I-SceI to replace *URA3ex* with the *LEU2ex* marker, yielding JMP1822. This plasmid was then digested with NotI to release the overexpression cassette.

Disruption or overexpression cassettes were used to transform the yeast via the lithium acetate method (30). Transformants were selected on YNB plus Leu medium or YNB medium, depending on the genotype. Genomic DNA from the transformants was prepared as described by Querol et al. (31). The corresponding ver1 and ver2 primers (Table 2) were used to verify *YlPEX11* and *TGL4* disruption. pTEF-Start and 61 stop primers were used to check the insertion of the overexpression cassettes *pTEF-YlPEX11-LEU2ex* and *pTEF-DGA2-LEU2ex*.

Restriction enzymes were obtained from Ozyme (Saint-Quentin-en-Yvelines, France). PCR amplifications were performed in an Eppendorf 2720 thermal cycler using GoTaq DNA polymerases (Promega, Madison, WI) for PCR verification and PyroBest DNA polymerases (TaKaRa, Saint-Germain-en-Laye, France) for cloning. PCR fragments were purified using a Qiagen purification kit (Hilden, Germany), and DNA fragments were recovered from agarose gels using a QIAquick gel extraction kit (Qiagen, Hilden, Germany). The amounts of DNA were measure with a MySpec (VWR, Fontenay-sous-Bois, France). All the reactions were performed in accordance with the manufacturer instructions. The Clone Manager software package was used for gene sequence analysis (Sci-Ed Software, Morrisville, NC).

Lipid determinations. Using 10- to 20-mg aliquots of freeze-dried cells, lipids were converted into their methyl esters by using the method described by Browse et al. (32). The esters produced were then used in gas chromatography (GC) analysis. The analysis was performed using a Varian 3900 gas chromatograph equipped with a flame ionization detector and a Varian FactorFour vf-23ms column, for which the bleed specification at 260°C was 3 pA (30 m, 0.25 mm, 0.25 μm). FAs were quantified using the internal standard method, which involved the addition of 50 μg of commercial $C_{17:0}$ (Sigma, Saint-Quentin Fallavier, France), and they were then identified by comparing their profiles to those for commercial FA methyl ester standards (FAME32; Supelco).

FFA and TAG determinations. Lipids from aliquots of 10 mg of cells were extracted by using the procedure of Folch et al. (33) for high-performance liquid chromatography (HPLC) analysis. Lipid species were analyzed using a gradient reversed-phase HPLC apparatus (Ultimate 3000; Dionex-Thermo Fisher Scientific, United Kingdom) and an Acclaim 120 C_8 3-μm 120 Å setup coupled to a Corona Veo detector. The column was eluted with a binary gradient solution (see Table S1 in the supplemental material) at 40°C and a constant flow rate of 0.8 ml min^{-1}. Identification and quantification were achieved via comparisons to standards.

Analysis of *YlPEX11*, *TGL4*, *DGA1*, *DGA2*, and *LRO1* expression. Precultures of the reference strain JMY2900 were placed in liquid YNB, supplemented with 1% glucose and 0.5% yeast extract, and grown for 15 h at 28°C. Cells were washed twice with distilled water and transferred to fresh liquid YNB medium supplemented with 1% glucose, 3% oleic acid, or both 1% glucose and 3% oleic acid. Cultures were incubated in baffled Erlenmeyer flasks at 28°C and 160 rpm. Cultures were harvested 2 and 6 h postinoculation, frozen in liquid nitrogen, and stored at −80°C. To determine the expression of *TGL4*, *DGA1*, *DGA2*, and *LRO1* in JMY2900 and Δ*YlPex11* grown in $YNBD_{0.5}O_3$, 10 ml of each culture was collected at different sampling times and centrifuged at 4,000 rpm for 5 min. Pellets were immediately frozen in liquid nitrogen and stored at −80°C. RNA was extracted from cells by using the RNeasy minikit (Qiagen, Hilden, Germany), and 2 μg was treated with DNase (Ambion, Life Technologies, Saint Aubin, France). cDNA was synthesized using the SuperScript III First-Strand reverse transcription-PCR (RT-PCR) kit (Invitrogen, Saint Aubin, France). PCR was then performed using the GoTaq DNA polymerase kit (Promega, Madison, WI) and employing specific primers designed by the Primer3 program (see Table 3, below). The actin- and alpha-1,2-mannosyltransferase-encoding genes (*Actin* and *ALG9*, respectively) were used as the controls.

TABLE 3 Shared identities of Pex11p proteins

Pex11p protein (size)	% shared identity with[a]: YlPex11p (233 aa)	YALI0C04565p (305 aa)	YALI0D25498p (299 aa)
AtPex11a (248 aa)	NF	NF	NF
AtPex11b (227 aa)	27 (5e−7)*	NF	NF
AtPex11c (235 aa)	24 (1e−4)	NF	NF
AtPex11d (236 aa)	26 (4e−5)*	NF	NF
AtPex11e (231 aa)	25 (1e−5)	NF	NF
HsPex11pα (247 aa)	23 (1e−15)	NF	NF
HsPex11pβ (259 aa)	20 (1e−11)	NF	NF
HsPex11pγ (241 aa)	NF	NF	NF
PcPex11pA (238 aa)	39 (3e−56)	NF	NF
PcPex11pB (224 aa)	18 (1e−6)	NF	NF
PcPex11pC (303 aa)	23 (1e−3)*	28 (1e−8)*	NF
PpPex11p (249 aa)	33 (1e−41)	NF	NF
ScPex11p (236 aa)	31 (2e−32)	NF	NF
YALI0C04565p (305 aa)	NF		NF
YALI0D25498p (299 aa)	NF	NF	
YlPex11p (233 aa)		NF	NF

[a] aa, amino acids; NF, not found. *, 55 to 60% coverage. E values are shown in parentheses.

Microscopic analysis. Images were acquired using a Zeiss Axio Imager M2 microscope (Zeiss, Le Pecq, France) capable of 100× magnification and equipped with Zeiss fluorescence microscopy filters 45 and 46. Axiovision 4.8 software (Zeiss, Le Pecq, France) was used to acquire images. Lipid bodies were stained by adding Bodipy lipid probe (2.5 mg/ml in ethanol; Invitrogen, Saint Aubin, France) to the cell suspension (A_{600} of 5) and letting the mixture incubate for 10 min at room temperature. The LIVE/DEAD BacLight bacterial viability kit (Life Technologies) was used as per the manufacturer's instructions to count living and dead cells under the microscope.

RESULTS AND DISCUSSION

Pex11p is conserved in *Yarrowia lipolytica*. *YALI0C04092* (*YlPEX11*) encodes a protein of 234 amino acids that shares 31% identity with ScPex11p, 33% identity with the Pex11p found in *Pichia pastoris* (PpPex11p), and 39% identity with the Pex11p found in *Penicillium chrysogenum* (PcPex11pA) (Table 3). This protein is also distantly related to human and plant Pex11p proteins (20 to 27% shared identities) (Table 3). Alignment of YlPex11p, ScPex11p, PpPex11p, and PcPex11pA showed that the N-terminal amphipathic helix described for PcPex11p is relatively well conserved (34) (Fig. 1A). This domain promotes the association between PcPex11p and liposomes *in vitro* and allows for membrane curvature (34); its presence in each of these four proteins suggests that the membrane-binding ability is also conserved. A Cys3 residue of ScPex11p involved in homodimerization (9) was found to be conserved in YlPex11p (residue Cys4) but not in PcPex11 or PpPex11 (Fig. 1). ScPex11p has been described as a protein that binds tightly to peroxisomal membranes (9), and it was not predicted by TMHMM to have a transmembrane domain (TM) (Fig. 1). Likewise, no TM was predicted for PpPex11p; however, two TMs were predicted for YlPex11p and PcPex11p

A

```
PpPex11p    MVLDTVVYHPTLDKVIQYLDSSAGRDKLLRLLQYLTKFVSFYLIKNGHSIVTAQTVRRIE 60
ScPex11p    MVCDTLVYHPSVTRFVKFLDGSAGREKVLRLLQYLARFLAVQNSS--------LLARQLQ 52
YlPex11p    -MSVCLAQNPTVTRVVKLLETHVGRDKILRSIQYFSRFLTYYLFRKGYTKDTIDIFRKIQ 59
PcPex11p    MVANTLVYHPALAHWLRFVATTVGRDKLLRTIQYFSRFYAWYLYRTNKPQSAIDPYNAVK 60
             :   :. :*:: : :: :   .**:*:** :**:::* :                . ::

PpPex11p    AIATLNRKALRFLKPLNHLKSASATFDNKLT-DKVTRYSQVLRDLGYAVYLALDSVSWFK 119
ScPex11p    AQFTTVRKFLRFLKPLNHLQAAAKFYDNKLASDNVVRVCNVLKNIFFAAYLSLDQVNLLR 112
YlPex11p    NQFSMARKLFRVGKPIGHLKTAAVSFENKT-LDPCLRYTTIGRNLGYAIYLVFDSIIYIN 118
PcPex11p    KQFGTTRKIMRIGKFLEHLKAAAVAFDNKSPVDPVLRYLAIGRQLGYAGYLTLDAVTVID 120
                  ** :*. * : **::*:  :**   *   *   : ::: :* ** :* :  :

PpPex11p    QLGISSTKRLP--QVQKLASLFWFVAVVGGAVNDLRKIRLSQQKVASLKQELVVTSDKEG 177
ScPex11p    ILKVIPVTVLTGKKIPRWSNWCWLFGLLSGLAMDLRKIQTSHAQIAAFVKAKSQSQGDEH 172
YlPex11p    GSGIKKIDNIK--TIKKVGSYFWAFGIFCNILNSIHKINICKKKRAALAAEKEKDTTSAK 176
PcPex11p    VIGIRKLSSAK--RLQDSAYRSWAAGLIFSTVAGIYTLVRLQEKEKTIDRKEGEGVVEAK 178
               :          :   .   *  .:. .   .: .:   : :  ::         .

PpPex11p    EQTVSKETINLIESESKLIGSTTITLIRDLLDGYIALNGFALQN-KDEKVGLAGVISSLI 236
ScPex11p    EDHKKVLGKAYQDRYTALR-----RLFWDAADSFIVLNNLGYLSSNEEYVALSGVVTSIL 227
YlPex11p    KNDKDAAAAQKQ-------------LVWDLLDFSIPLTSLGYLHLDDGLVGLAGFATGIM 223
PcPex11p    KIEKERSAARIQ-------------LISDVCDLAAPLSAVGILNLDDGIVGITGTISSLI 225
            :   .                    *. *  *    *. ..    .:  *.::*  :.::

PpPex11p    GIRDVWQGKYINE 249
ScPex11p    GMQDMWKAT---- 236
YlPex11p    GVQKAWAATA--- 233
PcPex11p    GVWSQWRKTAGPA 238
            *: . *  .
```

B

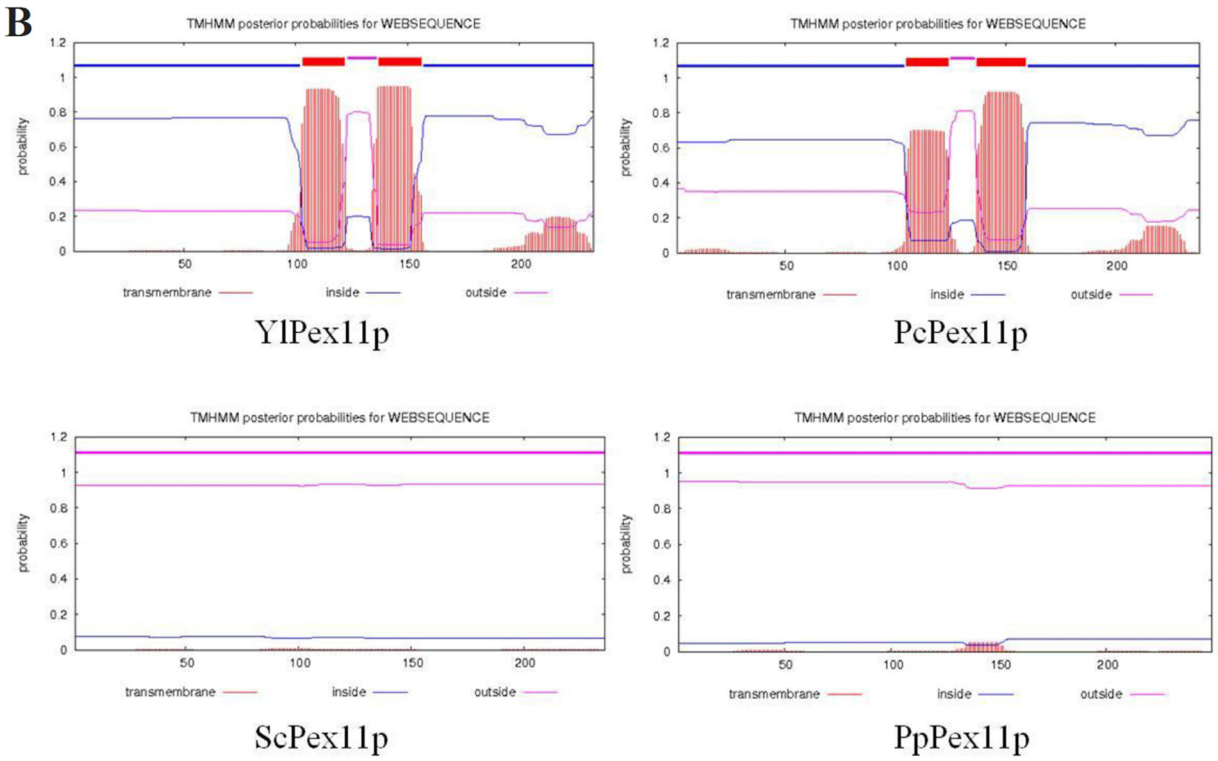

FIG 1 Analysis of YlPex11p, PcPex11p, PpPex11p, and ScPex11p proteins. (A) Alignment of YlPex11p (YALI0C04092p), PcPex11p (Pc12g09400p), PpPex11p (PP7435_Chr2-0790p), and ScPex11p (YOL147C) using ClustalW. Yl, *Y. lipolitica*, Sc, *S. cerevisiae*, Pc, *Penicillium chrysogenum*, Pp, *Pichia pastoris*. The amino acids in yellow are the transmembrane domains predicted by TMHMM. The black box encloses the pex11-Amph domain. The enlarged letters that are highlighted in gray indicate the location of the S165, S167, and C3 sites in ScPex11p, the putative phosphorylation sites S174 and C4 in YlPex11p, and the S173 site in PpPex11p. (B) TMHMM profiles of YlPex11p, PcPex11p, PpPex11p, and ScPex11p.

A

YALI0C04565p

MSLAYTVNLLRASGRLNKVLALLSNAGTLDPTLAFVGYGSLFVCELLRLESVQMGVVVAK
VLLGQVTGLDIDESFEKLGLASDLTGVADSLGVLSGLISDIRIFNRLWGLVGLISWGISE
YDAQQKPLDVNDPYIKYDKAVRVITALQVWSNLFYQPLENVAYLGMHKILPVSDAAQNSL
WLHSSKLWALHVVLELIRLVVEIRRNVKRQSIEKKAGKTTTTTDTKACNCTKLLPNFLKG
LGDQWWRDLVINLAYLPLTAHWSIDGGIVDNLIVGFLGASAAAANVGWKWKKALTPDVPV
EKKMQ

YALI0D25498p

MVSKLVGRTKPAGDSQKTVRIDEKVEIKEFQAHKPEIIDNTTEIPAPVPMSIAERSIADA
ARPPLHASPWRVFLTLFAEKGGLDKTIKLIQYTGRLLLWAAKQGWFTRHKQMMLLWKLAE
MESRLNGMVSNFSQFRKIIKLGEWLGPVEDLVTTKNPLTSLAFQSELMEVINTIGDDIYC
LSKIGVVKGKRLGRNGELMANWGWYGAIFINIKVGIETYQLAAKSGDEAAIWDAKLTLFK
LANDFIFCTIDCLEPEGLSNIYQTVTGLASGSVGFYKLWRKISKKLDKELEEKERCKTC

B

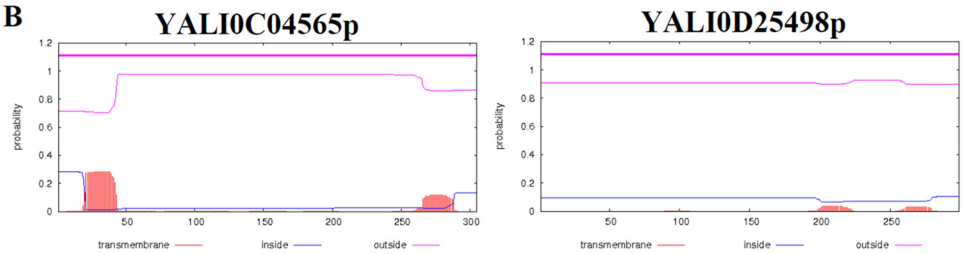

FIG 2 YALI0C04565p and YALI0D25498p sequences. (A) YALI0C04565p and YALI0D25498p sequences with the predicted Pex11 domain in gray. The putative dilysine motif (KKXX) is shown in red. (B) TMHMM profile.

(Fig. 1). Mammalian Pex11β and *Trypanosoma brucei* Pex11 each also contain two transmembrane domains (5, 35), suggesting that the structures of YlPex11p and PcPex11p are more similar to that of higher-eukaryote Pex11ps than to ScPex11p. Additionally, the phosphorylated residues S165 and S167 of ScPex11p (13) are not conserved in YlPex11p and PcPex11p, a finding that further highlights the divergence between ScPex11p and PcPex11p/YlPex11p. In fact, it appears that YlPex11p has only one serine at the potential phosphorylation position S174, and PcPex11p has none (Fig. 1). Similarly, it is known that PpPex11p is activated via phosphorylation at a single position, S173, by the fission machinery protein Fis1p (14). Interestingly, the three mammalian Pex11p proteins also interact with Fis1p (36, 37). However, no phosphorylation of Pex11pβ has been detected (38). All these data suggest that YlPex11p could be activated by the phosphorylation of Ser174, but it may also be the case that, as in mammals and *P. pastoris*, YlPex11p interacts with Fis1p (YALI0B06556p shares 48% of its identity with ScFis1p).

Moreover, in *S. cerevisiae*, the three other members of the Pex11p family appear to be involved in peroxisome division: ScPex25p recruits GTPase Rho1 to the peroxisome membrane, ScPex27p has an unknown function, and ScPex34p may possibly be a positive effector of peroxisome division (14, 18, 39). No homologues for these proteins were found in the genomes of *Y. lipolytica*, *P. chrysogenum*, or mammals such as *Mus musculus* or *Homo sapiens*, and the only *PEX25* homologues were found in *P. pastoris* (*PAS_chr3_0189* and *PP7435_Chr3-1041* in strains GS115 and CBS7435, respectively). However, it may be that other, undescribed proteins play a similar role as ScPex25p, ScPex27p, and ScPex34p. All these results suggest that the *S. cerevisiae* peroxisome division system is not completely conserved among eukaryotes. This is in agreement with the absence of complementation of Δ*Scpex11* by *YlPEX11* (data not shown).

***Yarrowia lipolytica* contains two other putative Pex11p proteins.** More interestingly, Kiel et al. (40) described two *Y. lipolytica* proteins, YALI0C04565p and YALI0D25498p, as potential Pex11 proteins. *In silico* analysis of these proteins showed that they are not homologues of YlPex11p, ScPex11p, PpPex11p, or PcPex11; instead, YALI0C04565p seems to be distantly related to PcPex11pC (Table 1). SMART (41, 42) indicated, at a low E value (9e−12), that YALI0C04565p contains a Pex11 domain (Fig. 2A, in gray). YALI0D25498p did not have any homologues in the nr database, but the conserved domain database (43) revealed that it does have a Pex11 domain (E value, 9.32e−6) (Fig. 2A, in gray). In contrast to its prediction for YlPex11, TMHMM did not predict any transmembrane domains for YALI0C04565p or YALI0D25498p (Fig. 2B). It may be that, similar to humans and *P. chrysogenum* (7, 44, 45) (Table 3), *Y. lipolytica* has multiple Pex11p proteins. As suggested by Kiel et al. (40), these two Pex11p-like proteins may play roles similar to those of ScPex25p and ScPex27p.

Interestingly, YALI0C04565p seems to have a dilysine motif at its C terminal (KKXX) (Fig. 2), just like AtPex11c, AtPex11d, AtPex11e, and HsPex11α (7, 8, 46). The dilysine motif (KXKXX or KKXX) has been shown to facilitate binding between peroxisomes and COP1 (coat protein complex I) (47), a protein complex which regulates membrane traffic in eukaryotic cells (48). This finding suggests that some Pex11 proteins may mediate peroxisome division via a coatomer-dependent type of membrane vesiculation. Indeed, trypanosome Pex11p and rat Pex11α, which each have a C-terminal dilysine motif, bind to coatomers (49). The

importance of the dilysine domain in Pex11p is still unclear. However, it is known that this domain is dispensable in the functioning of AtPex11e, trypanosome Pex11p, and rat Pex11α (7, 49). All these results suggest that *Y. lipolytica* is more similar to higher eukaryotes than to *S. cerevisiae* when it comes to peroxisome division.

YlPEX11 is induced by oleic acid. In *S. cerevisiae*, Pex11p plays a very important role for growth on oleic acid and is highly induced by this fatty acid (3, 4, 9). Because lipid metabolism is a key process in *Y. lipolytica*, we wanted to understand how the expression of the three putative *PEX11* genes, *YlPEX11*, *YALI0C04565*, and *YALI0D25498*, changed in response to oleic acid exposure in the reference strain JMY2900. Cells were grown on YNB (1% glucose) for 15 h and were then transferred into fresh liquid YNB media supplemented with 1% glucose ($YNBD_1$), 3% oleic acid ($YNBO_3$), or both 1% glucose and 3% oleic acid ($YNBD_1O_3$). Cells were harvested after 2 and 6 h of growth. RT-PCR analysis indicated that (i) *YlPEX11*, *YALI0C04565*, and *YALI0D25498* were expressed under all the conditions tested; (ii) as expected, *YlPEX11* was strongly upregulated in media containing oleic acid; and (iii) *YALI0C04565* and *YALI0D25498* were also strongly induced in oleic acid media, but their expression was lower at 6 h than at 2 h, especially in $YNBD_1O_3$ (Fig. 3). This result also showed that the presence of glucose did not affect the upregulation of *YlPEX11*, *YALI0C04565*, and *YALI0D25498* by oleic acid, showing that glucose catabolite repression does not exist in this yeast, contrary to *S. cerevisiae* (50). This suggests also that YlPex11p, YALI0C04565p, and YALI0D25498p could play highly important roles in breaking down oleic acid. In all subsequent experiments conducted in this study, we focused on *YlPEX11*, since it encodes the closest homologue of ScPex11p.

YlPEX11 deletion prevents growth on fatty acids. In *S. cerevisiae*, studies of ScPex11p's effects on growth on FA media have yielded mixed results. Erdmann and Blobel (3) and Huber et al. (11) found that Δ*Scpex11* was unable to grow on oleic acid, whereas Marshall et al. (4) and Rottensteiner et al. (12) showed that growth was possible. To better understand the general role of *YlPEX11* and to investigate the specific part it plays in FA oxidation, we created a knockout strain, JMY3227, and examined its ability to grow on media containing glucose and FAs of different chain lengths. No growth was observed on media containing most of the FAs tested here ($C_{10:0}$, $C_{14:0}$, $C_{16:0}$, and $C_{18:1}$), and only a low level of growth was observed on $C_{6:0}$ (Fig. 4). These results indicated that *YlPEX11* is essential for *Y. lipolytica* growth on FA media, regardless of FA chain length. By expressing *YlPEX11* using the strong promoter p*TEF* and thus complementing the missing function in Δ*Ylpex11* mutants, *Y. lipolytica* growth was restored on each of the FA media tested (Fig. 4). This result is consistent with the impaired growth of Δ*Scpex11* on MCFA reported by van Roermund et al. (10) and Rottensteiner et al. (12), as well as the failure of the deletion mutants to grow on oleic acid, as observed by Erdmann and Blobel (3) and Huber et al. (11). However, we cannot exclude the possibility that Δ*Ylpex11* failed to grow on the FA substrates because its peroxisomes lacked transport of essential proteins. In addition, this result demonstrates that Δ*Ylpex11* deletion was not compensated by the genomic copies of *YALI0C04565* and *YALI0D25498*. We hypothesize that YALI0C04565p and YALI0D25498p could have similar functions as ScPex25p and ScPex27p, which needs to be demonstrated. Indeed, in *S. cerevisiae*, the presence of the two latter genes does not compensate for the absence of *ScPEX11* (11, 12). Moreover, Δ*Ylpex11* exhibited impaired growth on glucose and YPD media that did not contain FAs (Fig. 4 and data not shown). This finding suggests that, in contrast to *S. cerevisiae*, *YlPEX11* in *Y. lipolytica* is important not only for FA oxidation but also for general growth.

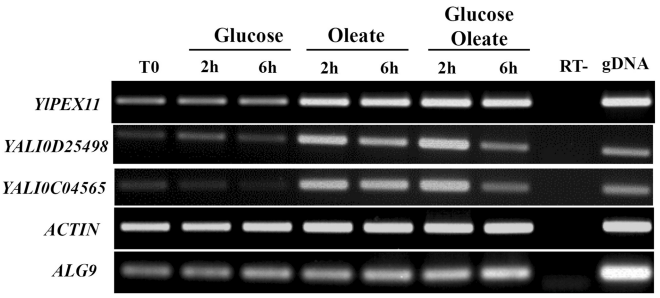

FIG 3 Expression profiles of *YlPEX11*, *YALI0C04565*, and *YALI0D25498* in the presence of glucose and oleic acid. Precultures were grown for 15 h at 28°C (T0) in liquid YNB supplemented with 1% glucose and 0.5% yeast extract; they were then transferred to fresh liquid YNB media supplemented with 1% glucose, 3% oleic acid, or both 1% glucose and 3% oleic acid. RT-PCR was performed on cells incubated for 2 and 6 h postinoculation. *Actin* and *ALG9* were used as endogenous controls for all the conditions tested.

Δ*Ylpex11* shows dose-dependent sensitivity to oleic acid. The fact that Δ*Ylpex11* failed to grow on oleic acid media could be due to a sensitivity to oleic acid. To determine the minimum concentration of oleic acid that inhibits Δ*Ylpex11* growth, JMY2900 and Δ*Ylpex11* were grown for 24 h in $YNBD_{0.5}$ media that contained different concentrations of oleic acid (from 0.1% to 3%). Cell survival was determined by running a drop test on YPD plates, and cell morphology was characterized by microscopy (Fig. 5). In the reference strain (JMY2900), the number and size of the lipid bodies increased as oleic acid concentrations increased; in Δ*Ylpex11*, cell morphology was increasingly affected by higher levels of oleic acid (Fig. 5A) and became noticeably different from that of the reference strain when oleic acid concentrations were greater than 0.5%. At oleic acid concentrations of 1% and 3%, several Δ*Ylpex11* cells appeared to lack vacuoles and lipid bodies, which are dead cells (bleary cells stained with Bodipy without a defined structure) (Fig. 5A). In accordance with the morphological observations, the drop test showed that Δ*Ylpex11* survival decreased with increasing levels of oleic acid (Fig. 5B; see also Fig. 8, below). Whereas JMY2900 and Δ*Ylpex11* had the same levels of survival in media containing 0.1% or 0.3% oleic acid ($YNBD_{0.5}O_{0.1}$ and $YNBD_{0.5}O_{0.3}$), Δ*Ylpex11* survival fell dramatically (500 to 1,000 times fewer normal-sized colonies than JMY2900) in media containing 0.5% to 3% oleic acid ($YNBD_{0.5}O_{0.5}$ and $YNBD_{0.5}O_3$) (Fig. 5B). These results showed that Δ*Ylpex11* is highly sensitive to oleic acid and that a concentration of 0.5% oleic acid is enough to strongly impact cell viability.

YlPEX11 is involved in peroxisome proliferation. In *S. cerevisiae*, plants, and mammals, Pex11 is involved in peroxisome fission, and giant peroxisomes are observed in Δ*pex11* mutants (3–8). In order to determine if this protein has the same function in *Y. lipolytica*, we generated mutants of the wild type and Δ*Ylpex11* that constitutively expressed a peroxisome-targeted RedStar2 fluorescent protein: JMY3175 (the wild-type JMY2900 with RedStar2SKL) and JMY3170 (the Δ*Ylpex11* strain expressing RedStar2SKL; RedStar2SKLp) (25). Experiments were performed in minimum media. In yeast grown on $YNBD_2$ (2% glucose), no peroxisomes were observed, probably because they were too small and/or too few in number to be visible (data not shown). However, in yeast grown on $YNBD_{0.5}O_3$, individual peroxisomes were

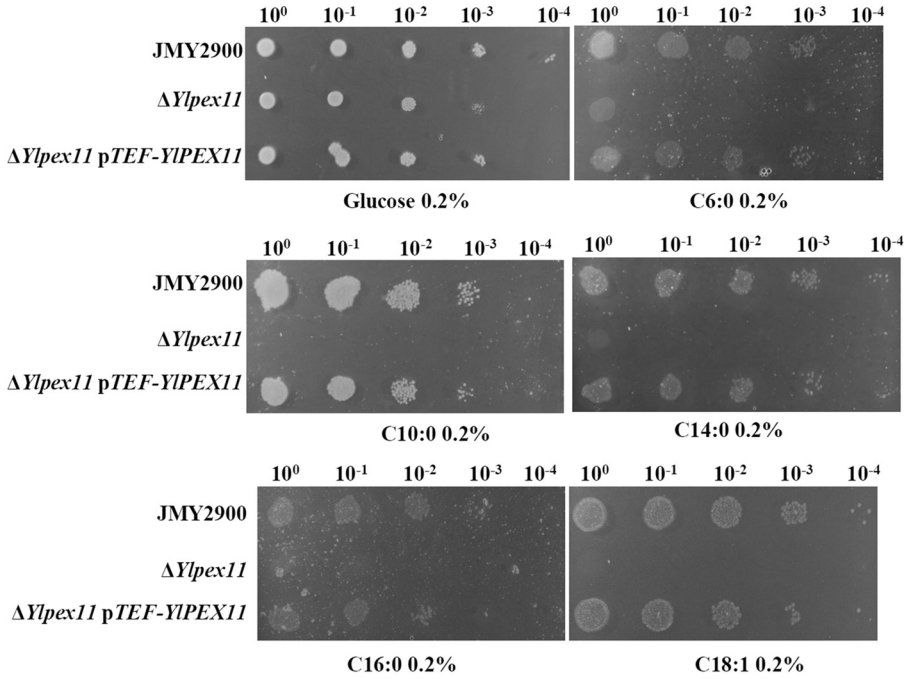

FIG 4 Growth of the reference strain JMY2900 and Δ*Ylpex11* strains on media containing glucose or fatty acids of different chain lengths. The carbon sources were as follows: glucose, methyl caproate ($C_{6:0}$), methyl decanoate ($C_{10:0}$), methyl myristate ($C_{14:0}$), methyl palmitate ($C_{16:0}$), and oleic acid ($C_{18:1}$). Pictures were taken after 2 or 3 days, and they are representative of 3 independent experiments.

easily distinguishable in JMY3165 (JMY330 p*TEF-RedStar2SKL*) but not in JMY3170 (Δ*Ylpex11* p*TEF-RedStar2SKL*). Instead, in JMY3170, red fluorescence increased rapidly overall and prevented accurate observation of peroxisomes, probably because the cells died too fast (data not shown). We therefore attempted a different strategy to observe the peroxisomes in JMY3170: 3% oleic acid ($YNBO_3$) was added to cells that had been previously grown for 16 h in $YNBD_2$. Because the oleic acid concentration

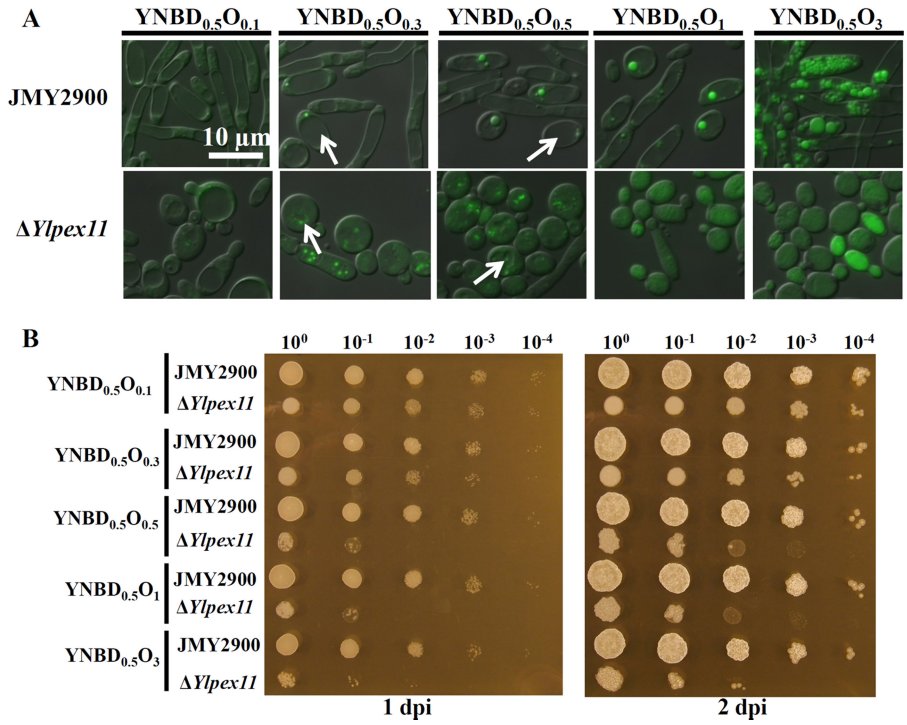

FIG 5 Phenotype of Δ*Ylpex11* cells grown in media containing different concentrations of oleic acid and glucose. (A) Microscopic images of the reference strain JMY2900 and Δ*Ylpex11*. Lipid bodies were stained with BodiPy. Arrows indicate the vacuoles. (B) Survival of Δ*Ylpex11* and the reference strain JMY2900 after 24 h of growth in different media. Before the dilutions, cells were adjusted to an OD_{600} of 1, and 5-μl drops were deposited on the YPD plates. dpi, days postinoculation.

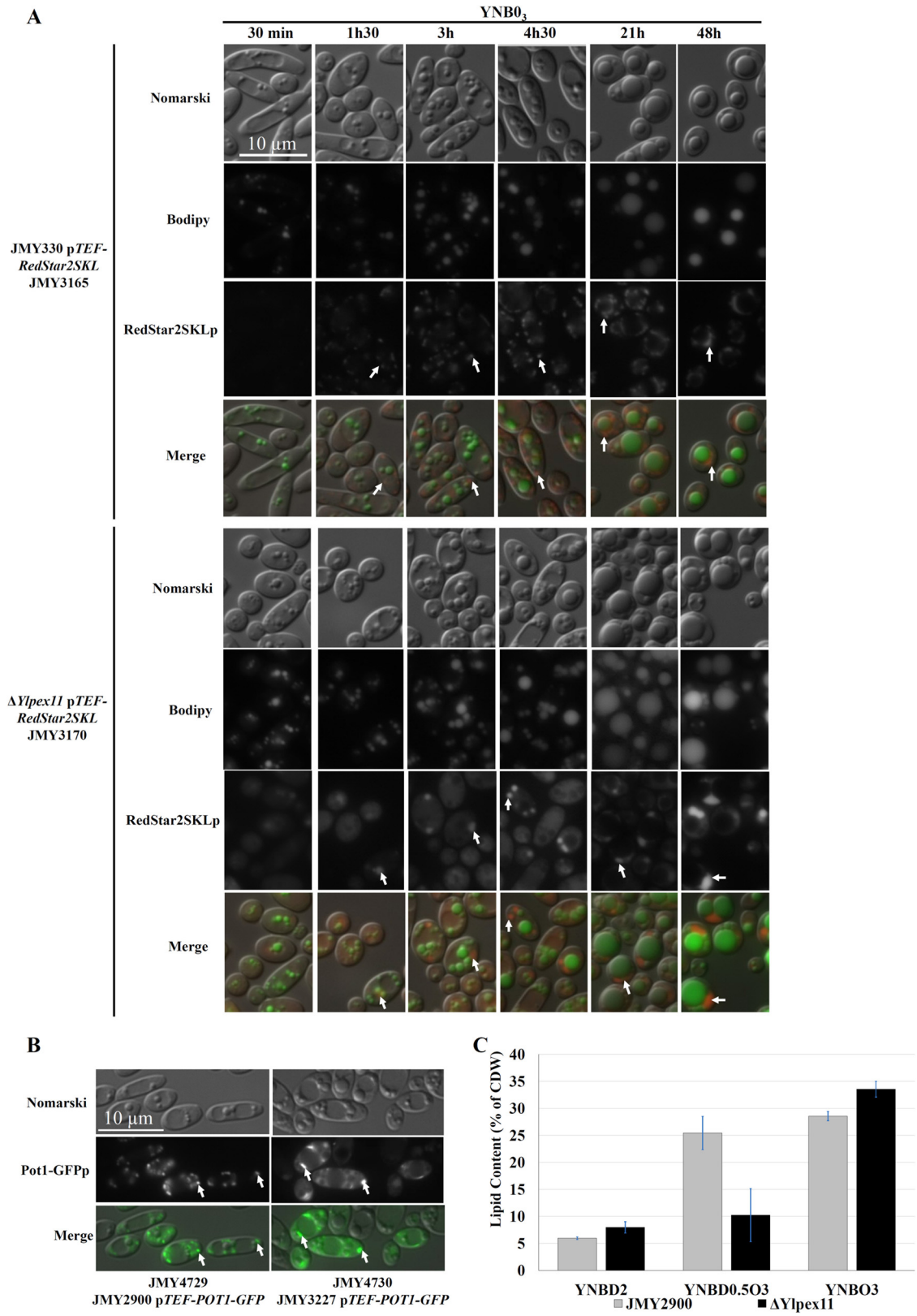

FIG 6 Microscopic images and lipid content of the wild type and Δ*Ylpex11*. (A) Morphology of JMY3175 (the wild-type JMY2900 with RedStar2SKLp) and JMY3170 (the Δ*Ylpex11* strain expressing RedStar2SKLp). Microscopic images are shown for cells cultivated for 16 h in YNBD to which 3% oleic acid was added ($YNBO_3$) at the indicated times after addition of oleic acid. Cell morphology was followed for a period of 48 h (30 min and 1.3, 3, 4.3, 21, and 48 h). Peroxisomes were stained red (RedStar2SKLp, rows 3 and 7), and lipid bodies were stained green (BodiPy, rows 2 and 6). White arrows indicate the peroxisomes. (B) Morphology of JMY4729 (the wild-type JMY2900 with Pot1-GFPp) and JMY4730 (the Δ*Ylpex11* strain with Pot1-GFPp). Microscopic images are of cells after 6 h of cultivation in YNBD to which 3% oleic acid was added. Peroxisomes were stained green (Pot1-GFPp). White arrows indicate the peroxisomes. (C) Total lipid content (FFAs and TAGs) as a percentage of yeast CDW. Analyses of total lipids were performed after 24 h for strains grown in $YNBD_2$ and $YNBD_{0.5}O_3$ and after 48 h for strains that experienced the addition of 3% oleic acid after having been grown in $YNBD_2$ ($YNBDO_3$). Gray bars, wild type; black bars, Δ*Ylpex11*.

TABLE 4 Lipid profiles

FA	% of FA in oleic acids	Relative % of FA in cells grown in $YNBD_{0.5}O_3$ (mean ± SD)	
		JMY2900	Δ*Ylpex11*
$C_{16:0}$	3.9	3.6 ± 0.2	4.2 ± 0.6
$C_{16:1(n-9)}$	0.9	2.7 ± 0.9	1.2 ± 0.3
$C_{16:1(n-7)}$	4.7	7 ± 1.9	3.4 ± 0.4
$C_{18:0}$	0.7	0.99 ± 0.1	0.8 ± 0.2
$C_{18:1(n-9)}$	73	68.4 ± 4.1	58 ± 8.7
$C_{18:2(n-6)}$	7	11 ± 2.2	17.4 ± 3.3

was low and we eliminated the glucose, it was thought that this process would slow down the growth, thus reducing Δ*Ylpex11* cell death due to oleic acid toxicity. One hour and 30 min after the addition of the oleic acid, the peroxisomes began to become visible in JMY3165 and JMY3170 cells (Fig. 6A, see particularly the panel for 4 h 30 min with RedStrad2SKLp). Whereas a dozen peroxisomes were visible in each JMY3165 cell, only a few giant peroxisomes (up to four) were visible in each JMY3170 cell (Fig. 6A, see particularly the results at 4 h 30 min, RedStrad2SKLp). The same results were obtained using Pot1-GFPp, a green fluorescent protein (GFP)-tagged 3-ketoacyl coenzyme A (CoA) thiolase used previously by Chang et al. (26) to stain peroxisomes. Small peroxisomes were stained in the wild type (JMY4729), while large peroxisomes were stained in the Δ*Ylpex11* strain (JMY4730) (Fig. 6B). These results strongly suggest that, as in other organisms, YlPex11p is involved in peroxisome fission and inheritance in *Y. lipolytica*. However, after 21 and 48 h of culture in $YNBO_3$, peroxisomes were physically closer to lipid bodies in both strains, probably to break down the FAs, but we cannot exclude that these results were caused by the size of lipid bodies that filled up most of the cells, changing the geometries of peroxisomes in cells.

The FA contents of the reference strain and Δ*Ylpex11* were analyzed using GC. The results revealed that FAs accounted for 6%, 25%, and 28% of JMY2900 cell dry weight (CDW) after 24 h or 48 h of growth on $YNBD_2$, $YNBD_{0.5}O_3$, and $YNBO_3$, respectively. In contrast, FAs accounted for 8%, 10%, and 33%, respectively, of Δ*Ylpex11* CDW under the same conditions (Fig. 6C). Notably, when exposed to nonlethal conditions ($YNBD_2$ and $YNBO_3$), Δ*Ylpex11* was able to accumulate more FAs than the reference strain. This higher total FA accumulation likely reflected the reduced β-oxidation activity in Δ*Ylpex11*. Indeed, the FA profiles of JMY2900 and Δ*Ylpex11*, obtained from strains grown on $YNBD_{0.5}O_3$, revealed some interesting differences. The main constituents of the oleic acids used in this study were the following: 73% $C_{18:1(n-9)}$, 7% $C_{18:2(n-6)}$, 4.7% $C_{16:1(n-7)}$, 3.9% $C_{16:0}$, and 0.9% $C_{16:1(n-9)}$ (Table 4). In JMY2900 cells, $C_{16:1(n-9)}$ accounted for 2.7% of the FAs, compared with the 0.9% present in the medium or the 1.2% present in Δ*Ylpex11* cells (Table 4). $C_{16:1(n-9)}$ cannot be synthesized by cells and is generated by the breakdown of $C_{18:1(n-9)}$. As the FAs that accumulate in *Y. lipolytica* cells generally reflect the FA composition of the extracellular medium (51), the overrepresentation of $C_{16:1(n-9)}$ in JMY2900 cells indicated that their β-oxidation was fully active. Similarly, the low level of $C_{16:1(n-9)}$ in Δ*Ylpex11* cells may indicate that β-oxidation, which produces this fatty acid by breaking down the $C_{18:1(n-9)}$ present in the medium, was not functional in this mutant. Moreover, $C_{18:2(n-6)}$ levels were proportionally higher in Δ*Ylpex11* than in JMY2900: that particular fatty acid represented 17% versus 11% of the total FAs, respectively (Table 4). In *Y. lipolytica*, $C_{18:2(n-6)}$ can be synthesized by the Δ12 fatty acid desaturase Fad2p, which converts $C_{18:1(n-9)}$ into $C_{18:2(n-6)}$. It is therefore possible that the very high level of $C_{18:2(n-6)}$ in Δ*Ylpex11* might have been due to the greater availability of $C_{18:1(n-9)}$ resulting from nonfunctional β-oxidation in this mutant.

To determine if YlPex11p is localized to peroxisomes as ScPex11p, a fusion protein was constructed at the C terminus by using YFP. This fusion was introduced into the JMY3170 (Δ*Ylpex11* p*TEF-RedStar2SKL*) derivative strain to create JMY2616 (Δ*Ylpex11* p*TEF-RedStar2SKL* p*TEF-YlPEX11-YFP*). We first analyzed the capacity of YlPex11-YFPp to complement the deletion of *YlPEX11* in a drop test on oleate medium. This protein is only partially functional, since JMY2616 grew slowly on oleate and colonies were smaller (Fig. 7A). Analysis of its localization showed that YlPex11-YFPp is localized at the periphery of peroxisomes (Fig. 7B), demonstrating that its localization is similar to that of ScPex11p at this time of induction.

It still remains unclear why Δ*Ylpex11* is unable to oxidize FAs. We previously showed that Δ*pox4* or Δ*pox5* (acyl-CoA oxidases) mutants, which also form giant peroxisomes, are still able to break down FAs (52). The failure of Δ*Ylpex11* to grow on oleic acid is thus not a simple consequence of having large peroxisomes. Furthermore, the observation that RedStar2SKLp (PTS1) and Pot1-GFPp (PTS2) correctly targeted the peroxisomes in the reference strain and the Δ*Ylpex11* mutant indicates that, even in the knockout yeast cells, proteins with PTS1 and PTS2 sequences remained correctly located in peroxisomes at this time of induction. However, we cannot exclude the possibility that other important proteins involved in β-oxidation were not imported into the peroxisomes.

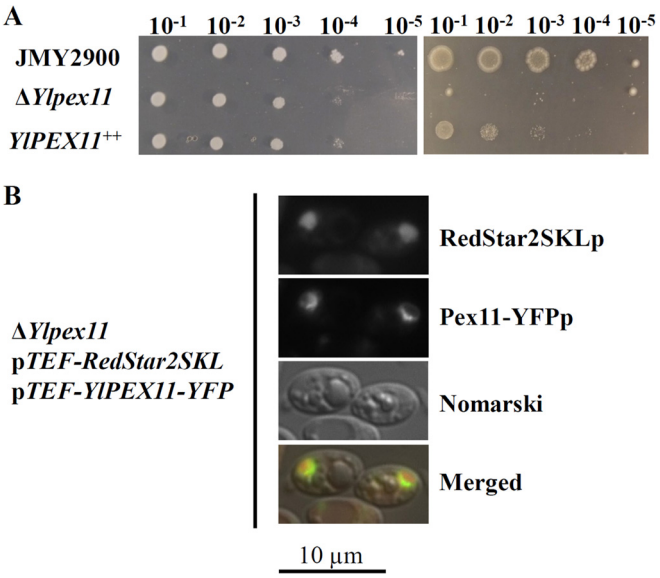

FIG 7 Complementation of Δ*Ylpex11* by overexpression of p*TEF-YlPEX11-YFP* and localization of YlPex11p-YFPp. (A) Growth of the reference strain JMY2900, Δ*Ylpex11*, and Δ*Ylpex11* p*TEF-RedStar2SKL* p*TEF-YlPEX11-YFP* strains on 0.2% glucose (left) or oleate (right) media. Pictures were taken after 2 and 5 days for glucose- or oleate-containing plates, respectively. (B) Localizations of RedStar2SKLp and YlPex11-YFPp observed after 4 h in $YNBDO_3$ medium.

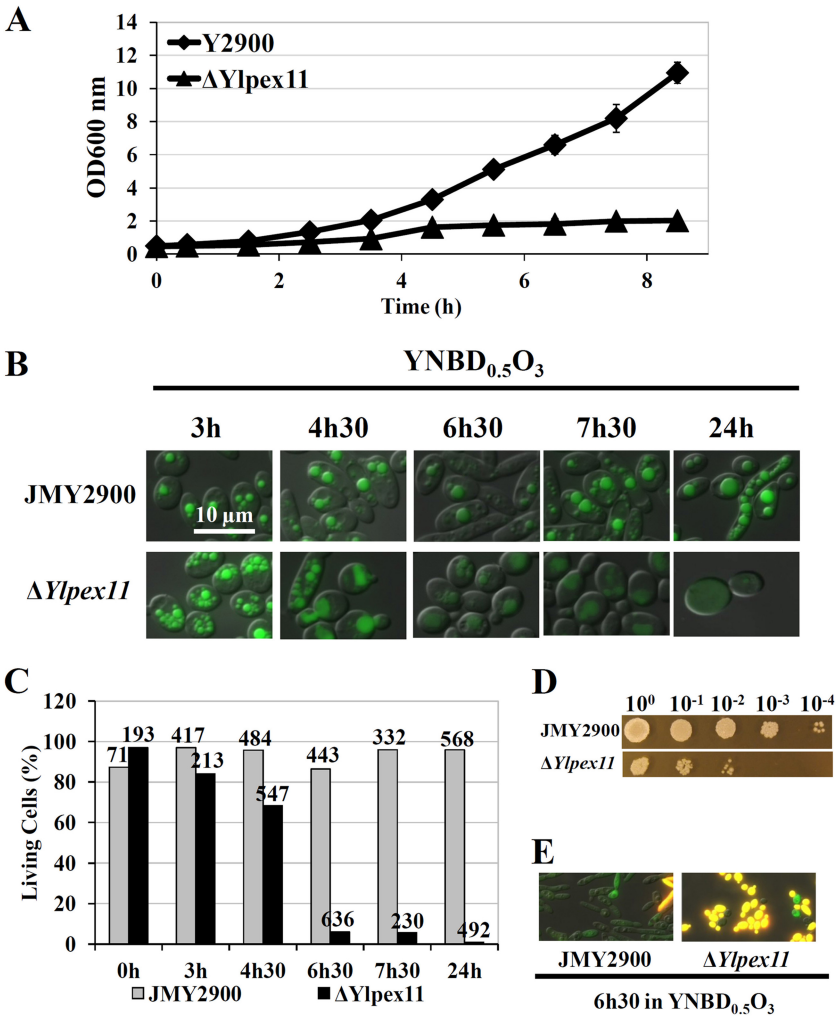

FIG 8 Phenotype of Δ*Ylpex11* grown in $YNBD_{0.5}O_3$ medium. (A) Growth curves of the reference strain JMY2900 and Δ*Ylpex11* cultured in $YNBD_{0.5}O_3$ medium. (B) Morphologies of the reference strain JMY2900 and Δ*Ylpex11* when grown in $YNBD_{0.5}O_3$. Lipid bodies were stained with BodiPy. (C) Survival of Δ*Ylpex11* grown in $YNBD_{0.5}O_3$, estimated using the LIVE/DEAD BacLight bacterial viability kit. Live and dead cells were counted, and the ratio of live cells to dead cells was calculated. The numbers above the bars are the total number of cells counted. (D) Survival of Δ*Ylpex11* after 24 h of growth in $YNBD_{0.5}O_3$. Before the dilutions, cells were adjusted to an OD_{600} of 1. Cells were grown for 2 days on YPD. (E) Example of cell coloration obtained using the LIVE/DEAD kit. Pictures were taken after cells had grown for 6 h 30 min in the $YNBD_{0.5}O_3$ medium. Green cells are alive, whereas yellow cells are dead.

YlPEX11 deletion affects the lipid body morphology of yeast grown in oleic acid media. To better understand why Δ*Ylpex11* did not survive when grown on FA media, we studied the morphology of cells grown on $YNBD_{0.5}O_3$ (Fig. 8). After 4 h 30 min of culture, Δ*Ylpex11* cells stopped growing (Fig. 8A), which suggests that oleic acid may inhibit the growth of this strain. Similar results have been obtained for *S. cerevisiae*: when Δ*Scpex11* was cultivated in the presence of oleic acid and galactose, it stopped growing after 8 h of culture (8). Under the microscope, Δ*Ylpex11*, after 3 h of growth, had a higher number of lipid bodies. However, at this time, we observed a typical shape (round) as with the reference strain, JMY2900 (Fig. 8B). However, after 4 h 30 min, Δ*Ylpex11* cells contained lipid bodies with seemingly modified shapes, and the lipid bodies appeared increasingly diffuse over time (Fig. 8B). At 24 h of growth, Δ*Ylpex11* cells had a round morphology; they were devoid of lipid bodies and vacuoles due to cell death (Fig. 8B). This phenotype has not been previously observed in mutants in which β-oxidation has been deleted, such as the Δ*pox1-6* mutant (51, 53) or the Δ*mfe* mutant (53, 54), which suggests that the lack of functional β-oxidation could not by itself be responsible for the phenotype we observed. The survival rate analysis indicated that, when Δ*Ylpex11* and the reference strain were grown on $YNBD_{0.5}O_3$, strain survival rates were similar after the first 3 h of culture (84% and 97% live cells, respectively). Survival stayed constant for the reference strain (85 to 96%) (Fig. 8C and D) but decreased dramatically for Δ*Ylpex11*: from 68% at 4 h 30 min of culture to 5% at 6 h 30 min and 7 h 30 min of culture, and finally to 1% at 24 h of culture (96-fold lower than the reference strain result) (Fig. 8C to E). These data were confirmed in a drop test (Fig. 8D). Taken together, these findings suggest that the Δ*Ylpex11* deletion mutant was not viable in the presence of oleic acid, probably due to improper lipid homeostasis (lipid body lysis).

Oleic acid toxicity may be due to profoundly altered triglyceride metabolism in yeast. One potential explanation for the appearance of diffuse lipid bodies in Δ*Ylpex11* (Fig. 8B) could be an increased remobilization of the triacylglycerols (TAGs) that make up most lipid bodies. Under this scenario, cell death would be caused by the liberation of FFAs into the cytoplasm. In order to better understand what happens when Δ*Ylpex11* is grown in $YNBD_{0.5}O_3$, the expression levels of genes involved in TAG storage (such as *DGA1*, *LRO1*, and particularly *DGA2* [23]) and TAG remobilization (such as *Tgl4p* [24, 53]) were analyzed using RT-

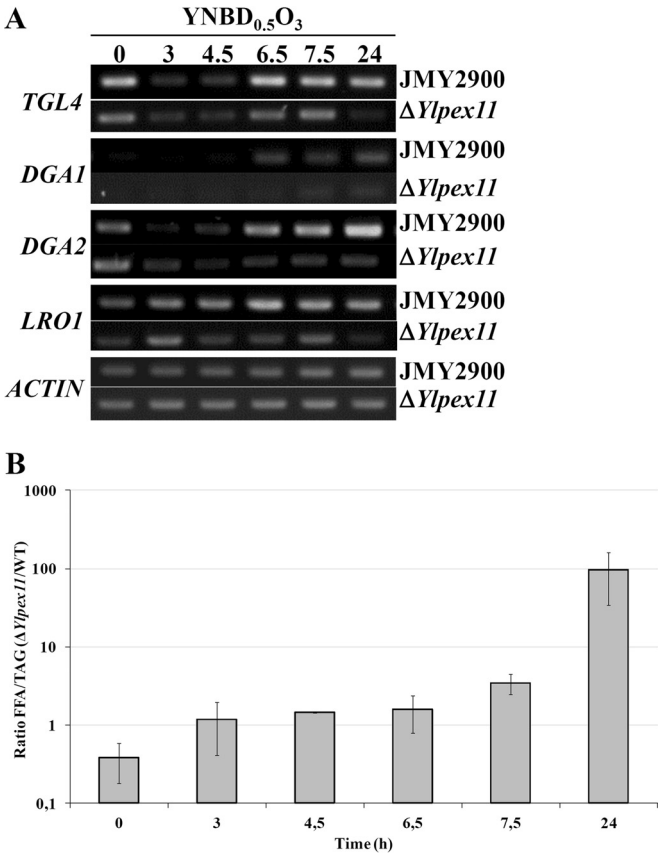

FIG 9 Impact of the deletion of *YlPEX11* on the expression of *TGL4*, *DGA1*, *DGA2*, and *LRO1* and on the FFA/TAG ratio during growth in $YNBD_{0.5}O_3$. (A) Expression of *TGL4*, *DGA1*, *DGA2*, and *LRO1* in JMY2900 and Δ*Ylpex11* strains. RT-PCR was performed at different times during 24 h of culture. *Actin* was used as the endogenous control. (B) The FFA/TAG ratios for Δ*Ylpex11* and JMY2900. HPLC was used to analyze these compounds.

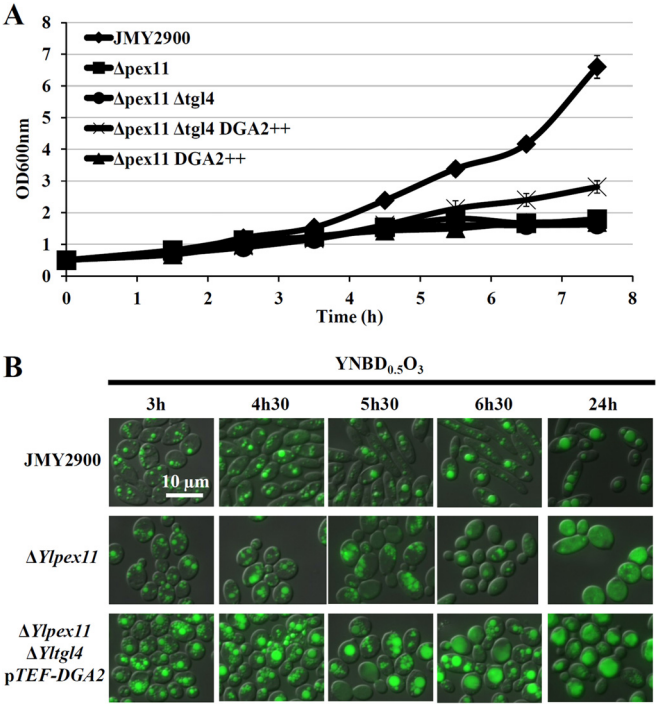

FIG 10 Phenotypes of Δ*Ylpex11*-derived strains grown in $YNBD_{0.5}O_3$ medium. (A) Growth curves of JMY2900, Δ*Ylpex11*, Δ*Ylpex11* Δ*Yltgl4*, Δ*Ylpex11* p*TEF-DGA2*, and Δ*Ylpex11* Δ*Yltgl4* p*TEF-DGA2* cultured in $YNBD_{0.5}O_3$. (B) Morphologies of JMY2900, Δ*Ylpex11*, and Δ*Ylpex11* Δ*Yltgl4* p*TEF-DGA2* grown in $YNBD_{0.5}O_3$. Lipid bodies were stained with BODIPY.

PCR (Fig. 9). Surprisingly, the global expression levels of *TGL4*, *DGA1*, *DGA2*, and *LRO1* were lower in Δ*Ylpex11* than in the reference strain, particularly at 24 h of growth (Fig. 9A). At 3 h of growth, expression levels of *TGL4*, *DGA1*, and *LRO1* were quite similar in JMY2900 and Δ*Ylpex11* cells (Fig. 9A). However, also at 3 h of growth, *DGA2* showed a higher level of expression in Δ*Ylpex11* cells, suggesting that TAG synthesis at this time was more active in Δ*Ylpex11* than it was in the reference strain (Fig. 9A). One possible explanation for this is that the decreased FA consumption in the mutant allowed for increased TAG storage. Interestingly, in JMY2900 after 4 h 30 min of growth, expression of *TGL4*, *DGA1*, and *LRO1* stayed stable and expression of *DGA2* increased, which resulted in TAG accumulation into the lipid bodies. In contrast, in Δ*Ylpex11*, expression of *DGA2* and *LRO1* decreased, suggesting that TAG synthesis decreased also, and FFA levels increased (Fig. 9A). After 6 h 30 min and 7 h 30 min of culture, the reference strain demonstrated increased expression of all four genes; in contrast, only *TGL4* expression increased in Δ*Ylpex11* (Fig. 9A). This pattern suggests that there was a change in lipid homeostasis in Δ*Ylpex11* that resulted in the presence of more and more FFAs in the cells, whereas in the reference strain, increased *TGL4* expression was probably compensated by increased *DGA1*, *DGA2*, and *LRO1* expression (Fig. 9A), leading to a greater level of TAGs. Analyses of the ratio of FFA versus TAG by HPLC between Δ*Ylpex11* and the reference strain confirmed this hypothesis. Indeed, the FFA/TAG ratio was increasing after 4 h 30 min of culture for Δ*Ylpex11* and reached 100-fold more than the wild type at 24 h (Fig. 9B). It may be that part of the cell death observed when Δ*Ylpex11* was grown on $YNBD_{0.5}O_3$ can be explained by the liberation of FFAs into the cytoplasm following lysis of the lipid bodies.

***TGL4* and *DGA2* are partially involved in lipid body lysis.** In *Y. lipolytica*, *DGA2* and *TGL4* are the most important genes regulating TAG synthesis and remobilization, respectively (19, 24). It is therefore likely that they play a role in the lysis of lipid bodies. To test this hypothesis, we created Δ*Ylpex11* strains in which *TGL4* was deleted and/or *DGA2* was overexpressed. The strains were grown in $YNBD_{0.5}O_3$, and their cell morphology was characterized using microscopy. While Δ*Ylpex11* Δ*tgl4* and Δ*Ylpex11* p*TEF-DGA2* had similar growth patterns as Δ*Ylpex11*, Δ*Ylpex11* Δ*tgl4* p*TEF-DGA2* demonstrated an intermediate growth pattern (Fig. 10A), suggesting that combining a *TGL4* deletion with *DGA2* overexpression partially rescued the Δ*Ylpex11* growth defect by reducing the strain's sensitivity to oleic acid. Microscopic observations of Δ*Ylpex11* Δ*tgl4* p*TEF-DGA2* grown in $YNBD_{0.5}O_3$ supported this hypothesis; indeed, lysis of the lipid bodies occurred 2 h later than in Δ*Ylpex11* (Fig. 10B). In addition, we observed a multiplicity of small lipid bodies surrounding a large lipid body. Moreover, the drop test indicated that Δ*Ylpex11* Δ*tgl4* p*TEF-DGA2* cultivated in $YNBD_{0.5}O_3$ grew faster than Δ*Ylpex11* on YPD plates (data not shown). However, in Δ*Ylpex11* at 24 h of growth, neither *TGL4* deletion nor *DGA2* overexpression prevented cell

death (Fig. 10B and data not shown). Interestingly, the lipid bodies conserved a shape (albeit not corresponding to that of the wild type, JMY2900) which suggested that *TGL4* deletion and *DGA2* overexpression counteracted lipid body lysis but were not able to fully prevent it from occurring. Therefore, other genes are probably involved in the cell death of Δ*Ylpex11* grown in oleic acid media.

Conclusions. The aim of this study was to explore the role played by Pex11p in the oleaginous yeast *Y. lipolytica*. Studies with *S. cerevisiae* have yielded mixed results regarding Δ*Scpex11* growth on oleic acid; indeed, two previous studies that used the same strain, UTL-7A, had contradictory results (3, 12). We demonstrated here that Δ*Ylpex11* was unable to grow on FA media, suggesting that Pex11p is essential in allowing *Y. lipolytica* to grow on oleic acid. As in other organisms (3–8, 10, 33, 55), YlPex11p is necessary for peroxisome fission, and therefore the deletion of *Ylpex11* generates giant peroxisomes when yeast are grown in minimum oleic acid medium. In our study, these giant peroxisomes were able to transport RedStar2SKLp or Pot1-GFPp, an observation which suggests that, despite other changes to peroxisome function, all the proteins containing a PTS1 (SKL) or PTS2 [(R,K)-(L,V,I)-X5-(H,Q)-(L,A,F) close to the N terminal, such as Pot1p] sequences were still correctly addressed to the peroxisome in minimum media. In addition to the difference in growth on oleic acid media, three other factors suggest that *S. cerevisiae* and *Y. lipolytica* have distinct peroxisome fission mechanisms: (i) putative phosphorylation sites differ between YlPex11p and ScPex11p; (ii) *Y. lipolytica* has two distinct Pex11-like proteins (YALI0C04565p and YALI0D25498p); (iii) *Y. lipolytica* lacks homologues of the Pex25p, Pex27p, and Pex34p proteins found in *S. cerevisiae*. It seems likely that increased understanding of peroxisome fission in *Y. lipolytica* could be a promising line of research in the near future, especially because the peroxisome fission mechanism of *Y. lipolytica* is more similar to that in higher eukaryotes than in *S. cerevisiae*. Cell death of Δ*Ylpex11* mutants grown on minimum and rich oleic acid media may be mediated by an alteration of lipid homeostasis resulting in an increase of the FFA/TAG ratio and a modification of lipid body morphology that probably results in the release of FFAs into the cytoplasm. The underlying cause of the lipid body lysis is still not well understood, but it may involve *TGL4* and *DGA2*. An imbalance in their expression (*TGL4* being overexpressed relative to *DGA2*) may contribute to the breakdown of lipid bodies, ultimately leading to their lysis. Indeed, *TGL4* deletion coupled with *DGA2* overexpression partially protected Δ*Ylpex11* against oleic acid toxicity, delaying cell death. Lipid homeostasis could also perturb sphingolipid metabolism. Sphingolipids are involved in a variety of biological processes, and the metabolites of these sphingolipids, such as ceramide, sphingosine, and sphingosine-1-phosphate, can regulate apoptosis (56). This could explain why the overexpression of *DGA2* and deletion of *TGL4* are not sufficient to save the phenotype of Δ*Ylpex11*. All these results demonstrate that YlPex11p is involved in lipid homeostasis in *Y. lipolytica* and that further research should be carried out in the near future to better understand the role of YlPex11p in this process.

During the revision of the manuscript, complementary work on *PEX11* function was performed in rich media and showed a defect in peroxisome biogenesis and a defect in the targeting of peroxisomal proteins (57). However, those authors did not report the effect on lipid body structure or number, in either the Δ*Ylpex11* cells showing abnormal small lipid bodies or in the Δ*Ylpex11* strain complemented by overexpression of *YlPEX11*, which showed large egg-shaped lipid bodies.

Taken together, these results show that Pex11p is involved in lipid homeostasis, maybe by connecting peroxisome biogenesis, lipid storage, and lipid remobilization. Further experiments have to be performed in minimum media containing lower oleic acid concentrations to reduce the effects of peroxisomal protein targeting and the effect of oleic acid toxicity.

ACKNOWLEDGMENTS

This work was supported by FIDOP/FASO funds (Fonds d'action stratégique des oléagineux) from the French vegetable oil and protein production industry.

We thank R. Rachubinski for the pUB4-p*TEF-POT1-GFP* vector. We also thank T. Rossignol for plasmid JMP1822 and C. Gaillardin for his helpful comments. We also thank J. Pearce and L. Higgins for their language editing services.

REFERENCES

1. **Kunau WH, Bühne S, de la Garza M, Kionka C, Mateblowski M, Schultz-Borchard U, Thieringer R.** 1988. Comparative enzymology of beta-oxidation. Biochem Soc Trans **16:**418–420.
2. **Kohlwein SD, Veenhuis M, van der Klei IJ.** 2013. Lipid droplets and peroxisomes: key players in cellular lipid homeostasis or a matter of fat—store 'em up or burn 'em down. Genetics **193:**1–50. http://dx.doi.org/10.1534/genetics.112.143362.
3. **Erdmann R, Blobel G.** 1995. Giant peroxisomes in oleic acid-induced *Saccharomyces cerevisiae* lacking the peroxisomal membrane protein Pmp27p. J Cell Biol **128:**509–523. http://dx.doi.org/10.1083/jcb.128.4.509.
4. **Marshall PA, Krimkevich YI, Lark RH, Dyer JM, Veenhuis M, Goodman JM.** 1995. Pmp27 promotes peroxisomal proliferation. J Cell Biol **129:**345–355. http://dx.doi.org/10.1083/jcb.129.2.345.
5. **Abe I, Fujiki Y.** 1998. cDNA cloning and characterization of a constitutively expressed isoform of the human peroxin Pex11p. Biochem Biophys Res Commun **252:**529–533. http://dx.doi.org/10.1006/bbrc.1998.9684.
6. **Li X, Gould SJ.** 2002. *PEX11* promotes peroxisome division independently of peroxisome metabolism. J Cell Biol **156:**643–651. http://dx.doi.org/10.1083/jcb.200112028.
7. **Lingard MJ, Trelease RN.** 2006. Five *Arabidopsis* peroxin 11 homologs individually promote peroxisome elongation, duplication or aggregation. J Cell Sci **119:**1961–1972. http://dx.doi.org/10.1242/jcs.02904.
8. **Orth T, Reumann S, Zhang X, Fan J, Wenzel D, Quan S, Hu J.** 2007. The PEROXIN11 protein family controls peroxisome proliferation in *Arabidopsis*. Plant Cell **19:**333–350. http://dx.doi.org/10.1105/tpc.106.045831.
9. **Marshall PA, Dyer JM, Quick ME, Goodman JM.** 1996. Redox-sensitive homodimerization of Pex11p: a proposed mechanism to regulate peroxisomal division. J Cell Biol **135:**123–137. http://dx.doi.org/10.1083/jcb.135.1.123.
10. **van Roermund CW, Tabak HF, van Den Berg M, Wanders RJ, Hettema EH.** 2000. Pex11p plays a primary role in medium-chain fatty acid oxidation, a process that affects peroxisome number and size in *Saccharomyces cerevisiae*. J Cell Biol **150:**489–498. http://dx.doi.org/10.1083/jcb.150.3.489.
11. **Huber A, Koch J, Kragler F, Brocard C, Hartig A.** 2012. A subtle interplay between three Pex11 proteins shapes de novo formation and fission of peroxisomes. Traffic **13:**157–167. http://dx.doi.org/10.1111/j.1600-0854.2011.01290.x.
12. **Rottensteiner H, Stein K, Sonnenhol E, Erdmann R.** 2003. Conserved function of pex11p and the novel pex25p and pex27p in peroxisome biogenesis. Mol Biol Cell **14:**4316–4328. http://dx.doi.org/10.1091/mbc.E03-03-0153.
13. **Knoblach B, Rachubinski RA.** 2010. Phosphorylation-dependent activation of peroxisome proliferator protein *PEX11* controls peroxisome abundance. J Biol Chem **285:**6670–6680. http://dx.doi.org/10.1074/jbc.M109.094805.
14. **Joshi S, Agrawal G, Subramani S.** 2012. Phosphorylation-dependent Pex11p and Fis1p interaction regulates peroxisome division. Mol Biol Cell **23:**1307–1315. http://dx.doi.org/10.1091/mbc.E11-09-0782.
15. **Pan R, Hu J.** 2011. The conserved fission complex on peroxisomes and mitochondria. Plant Signal Behav **6:**870–872. http://dx.doi.org/10.4161/psb.6.6.15241.

16. **Smith JJ, Marelli M, Christmas RH, Vizeacoumar FJ, Dilworth DJ, Ideker T, Galitski T, Dimitrov K, Rachubinski RA, Aitchison JD.** 2002. Transcriptome profiling to identify genes involved in peroxisome assembly and function. J Cell Biol **158:**259–271. http://dx.doi.org/10.1083/jcb.200204059.
17. **Tam YY, Torres-Guzman JC, Vizeacoumar FJ, Smith JJ, Marelli M, Aitchison JD, Rachubinski RA.** 2003. Pex11-related proteins in peroxisome dynamics: a role for the novel peroxin Pex27p in controlling peroxisome size and number in *Saccharomyces cerevisiae*. Mol Biol Cell **14:**4089–4102. http://dx.doi.org/10.1091/mbc.E03-03-0150.
18. **Tower RJ, Fagarasanu A, Aitchison JD, Rachubinski RA.** 2011. The peroxin Pex34p functions with the Pex11 family of peroxisomal divisional proteins to regulate the peroxisome population in yeast. Mol Biol Cell **22:**1727–1738. http://dx.doi.org/10.1091/mbc.E11-01-0084.
19. **Beopoulos A, Nicaud JM, Gaillardin C.** 2011. An overview of lipid metabolism in yeasts and its impact on biotechnological processes. Appl Microbiol Biotechnol **90:**1193–1206. http://dx.doi.org/10.1007/s00253-011-3212-8.
20. **Liu H, Tan X, Veenhuis M, McCollum D, Cregg JM.** 1992. An efficient screen for peroxisome-deficient mutants of *Pichia pastoris*. J Bacteriol **174:**4943–4951.
21. **Barth G, Gaillardin C.** 1996. *Yarrowia lipolytica*, p 313–388. *In* Wolf K (ed), Nonconventional yeasts in biotechnology: a handbook. Springer, Berlin, Germany.
22. **Haddouche R, Delessert S, Sabirova J, Neuvéglise C, Poirier Y, Nicaud JM.** 2010. Roles of multiple acyl-CoA oxidases in the routing of carbon flow towards β-oxidation and polyhydroxyalkanoate biosynthesis in *Yarrowia lipolytica*. FEMS Yeast Res **10:**917–927. http://dx.doi.org/10.1111/j.1567-1364.2010.00670.x.
23. **Beopoulos A, Haddouche R, Kabran P, Dulermo T, Chardot T, Nicaud JM.** 2012. Identification and characterization of *DGA2*, an acyltransferase of the *DGAT1* acyl-CoA:diacylglycerol acyltransferase family in the oleaginous yeast *Yarrowia lipolytica*. New insights into the storage lipid metabolism of oleaginous yeasts. Appl Microbiol Biotechnol **93:**1523–1537. http://dx.doi.org/10.1007/s00253-011-3506-x.
24. **Dulermo T, Tréton B, Beopoulos A, Kabran Gnankon AP, Haddouche R, Nicaud JM.** 2013. Characterization of the two intracellular lipases of *Y. lipolytica* encoded by *TGL3* and *TGL4* genes: new insights into the role of intracellular lipases and lipid body organisation. Biochim Biophys Acta **1831:**1486–1495. http://dx.doi.org/10.1016/j.bbalip.2013.07.001.
25. **Kabran P, Rossignol T, Gaillardin C, Nicaud JM, Neuvéglise C.** 2012. Alternative splicing regulates targeting of malate dehydrogenase in *Yarrowia lipolytica*. DNA Res **19:**231–244. http://dx.doi.org/10.1093/dnares/dss007.
26. **Chang J, Fagarasanu A, Rachubinski RA.** 2007. Peroxisomal peripheral membrane protein Yllnp1p is required for peroxisome inheritance and influences the dimorphic transition in the yeast *Yarrowia lipolytica*. Eukaryot Cell **6:**1528–1537. http://dx.doi.org/10.1128/EC.00185-07.
27. **Sambrook J, Maniatis T, Fritsch EF.** 1989. Molecular cloning: a laboratory manual, 2nd ed. Cold Spring Harbor Laboratory, Cold Spring Harbor, NY.
28. **Mlícková K, Roux E, Athenstaedt K, d'Andrea S, Daum G, Chardot T, Nicaud JM.** 2004. Lipid accumulation, lipid body formation, and acyl coenzyme A oxidases of the yeast *Yarrowia lipolytica*. Appl Environ Microbiol **70:**3918–3924. http://dx.doi.org/10.1128/AEM.70.7.3918-3924.2004.
29. **Fickers P, Le Dall MT, Gaillardin C, Thonart P, Nicaud JM.** 2003. New disruption cassettes for rapid gene disruption and marker rescue in the yeast *Yarrowia lipolytica*. J Microbiol Methods **55:**727–737. http://dx.doi.org/10.1016/j.mimet.2003.07.003.
30. **Le Dall MT, Nicaud JM, Gaillardin C.** 1994. Multiple-copy integration in the yeast *Yarrowia lipolytica*. Curr Genet **26:**38–44. http://dx.doi.org/10.1007/BF00326302.
31. **Querol A, Barrio E, Huerta T, Ramón D.** 1992. Molecular monitoring of wine fermentations conducted by active dry yeast strains. Appl Environ Microbiol **58:**2948–2953.
32. **Browse J, McCourt PJ, Somerville CR.** 1986. Fatty acid composition of leaf lipids determined after combined digestion and fatty acid methyl ester formation from fresh tissue. Anal Biochem **152:**141–145. http://dx.doi.org/10.1016/0003-2697(86)90132-6.
33. **Folch J, Lees M, Sloane Stanley GH.** 1957. A simple method for the isolation and purification of total lipides from animal tissues. J Biol Chem **226:**497–509.
34. **Opaliński L, Kiel JA, Williams C, Veenhuis M, van der Klei IJ.** 2011. Membrane curvature during peroxisome fission requires Pex11. EMBO J **30:**5–16. http://dx.doi.org/10.1038/emboj.2010.299.
35. **Lorenz P, Maier AG, Baumgart E, Erdmann R, Clayton C.** 1998. Elongation and clustering of glycosomes in *Trypanosoma brucei* overexpressing the glycosomal Pex11p. EMBO J **17:**3542–3555. http://dx.doi.org/10.1093/emboj/17.13.3542.
36. **Kobayashi S, Tanaka A, Fujiki Y.** 2007. Fis1, DLP1, and Pex11p coordinately regulate peroxisome morphogenesis. Exp Cell Res **313:**1675–1686. http://dx.doi.org/10.1016/j.yexcr.2007.02.028.
37. **Koch J, Pranjic K, Huber A, Ellinger A, Hartig A, Kragler F, Brocard C.** 2010. *PEX11* family members are membrane elongation factors that coordinate peroxisome proliferation and maintenance. J Cell Sci **123:**3389–3400. http://dx.doi.org/10.1242/jcs.064907.
38. **Bonekamp NA, Grille S, Cardoso MJ, Almeida M, Aroso M, Gomes S, Magalhaes AC, Ribeiro D, Islinger M, Schrader M.** 2013. Self-interaction of human Pex11pβ during peroxisomal growth and division. PLoS One **8:**e53424. http://dx.doi.org/10.1371/journal.pone.0053424.
39. **Marelli M, Smith JJ, Jung S, Yi E, Nesvizhskii AI, Christmas RH, Saleem RA, Tam YY, Fagarasanu A, Goodlett DR, Aebersold R, Rachubinski RA, Aitchison JD.** 2004. Quantitative mass spectrometry reveals a role for the GTPase Rho1p in actin organization on the peroxisome membrane. J Cell Biol **167:**1099–1112. http://dx.doi.org/10.1083/jcb.200404119.
40. **Kiel JA, Veenhuis M, van der Klei IJ.** 2006. PEX genes in fungal genomes: common, rare or redundant. Traffic **7:**1291–1303. http://dx.doi.org/10.1111/j.1600-0854.2006.00479.x.
41. **Schultz J, Milpetz F, Bork P, Ponting CP.** 1998. SMART, a simple modular architecture research tool: identification of signaling domains. Proc Natl Acad Sci U S A **95:**5857–5864. http://dx.doi.org/10.1073/pnas.95.11.5857.
42. **Letunic I, Doerks T, Bork P.** 2012. SMART 7: recent updates to the protein domain annotation resource. Nucleic Acids Res **40:**D302–D305. http://dx.doi.org/10.1093/nar/gkr931.
43. **Marchler-Bauer A, Anderson JB, Derbyshire MK, DeWeese-Scott C, Gonzales NR, Gwadz M, Hao L, He S, Hurwitz DI, Jackson JD, Ke Z, Krylov D, Lanczycki CJ, Liebert CA, Liu C, Lu F, Lu S, Marchler GH, Mullokandov M, Song JS, Thanki N, Yamashita RA, Yin JJ, Zhang D, Bryant SH.** 2007. CDD: a conserved domain database for interactive domain family analysis. Nucleic Acids Res **35:**D237–D240. http://dx.doi.org/10.1093/nar/gkl951.
44. **Opaliński L, Veenhuis M, van der Klei IJ.** 2011. Peroxisomes: membrane events accompanying peroxisome proliferation. Int J Biochem Cell Biol **43:**847–851. http://dx.doi.org/10.1016/j.biocel.2011.03.006.
45. **Schrader M, Bonekamp NA, Islinger M.** 2012. Fission and proliferation of peroxisomes. Biochim Biophys Acta **1822:**1343–1357. http://dx.doi.org/10.1016/j.bbadis.2011.12.014.
46. **Yan M, Rayapuram N, Subramani S.** 2005. The control of peroxisome number and size during division and proliferation. Curr Opin Cell Biol **17:**376–383. http://dx.doi.org/10.1016/j.ceb.2005.06.003.
47. **Cosson P, Letourneur F.** 1997. Coatomer (COPI)-coated vesicles: role in intracellular transport and protein sorting. Curr Opin Cell Biol **9:**484–487. http://dx.doi.org/10.1016/S0955-0674(97)80023-3.
48. **Brandizzi F, Barlowe C.** 2013. Organization of the ER-Golgi interface for membrane traffic control. Nat Rev Mol Cell Biol **14:**382–392. http://dx.doi.org/10.1038/nrm3588.
49. **Maier AG, Schulreich S, Bremser M, Clayton C.** 2000. Binding of coatomer by the PEX11 C-terminus is not required for function. FEBS Lett **484:**82–86. http://dx.doi.org/10.1016/S0014-5793(00)02132-3.
50. **Gancedo JM.** 1998. Yeast carbon catabolite repression. Microbiol Mol Biol Rev **62:**334–361.
51. **Guo T, Kit YY, Nicaud JM, Le Dall MT, Sears SK, Vali H, Chan H, Rachubinski RA, Titorenko VI.** 2003. Peroxisome division in the yeast *Yarrowia lipolytica* is regulated by a signal from inside the peroxisome. J Cell Biol **162:**1255–1266. http://dx.doi.org/10.1083/jcb.200305055.
52. **Beopoulos A, Mrozova Z, Thevenieau F, Le Dall MT, Hapala I, Papanikolaou S, Chardot T, Nicaud JM.** 2008. Control of lipid accumulation in the yeast *Yarrowia lipolytica*. Appl Environ Microbiol **74:**7779–7789. http://dx.doi.org/10.1128/AEM.01412-08.
53. **Dulermo T, Nicaud JM.** 2011. Involvement of the G3P shuttle and β-oxidation pathway in the control of TAG synthesis and lipid accumulation in *Yarrowia lipolytica*. Metab Eng **13:**482–491. http://dx.doi.org/10.1016/j.ymben.2011.05.002.
54. **Haddouche R, Poirier Y, Delessert S, Sabirova J, Pagot Y, Neuvéglise C,**

Nicaud JM. 2011. Engineering polyhydroxyalkanoate content and monomer composition in the oleaginous yeast *Yarrowia lipolytica* by modifying the ß-oxidation multifunctional protein. Appl Microbiol Biotechnol **91:** 1327–1340. http://dx.doi.org/10.1007/s00253-011-3331-2.

55. **Schrader M, Reuber BE, Morrell JC, Jimenez-Sanchez G, Obie C, Stroh TA, Valle D, Schroer TA, Gould SJ.** 1998. Expression of PEX11beta mediates peroxisome proliferation in the absence of extracellular stimuli. J Biol Chem **273:**29607–29614. http://dx.doi.org/10.1074/jbc.273.45.29607.

56. **Van Brocklyn JR, Williams JB.** 2012. The control of the balance between ceramide and sphingosine-1-phosphate by sphingosine kinase: oxidative stress and the seesaw of cell survival and death. Comp Biochem Physiol **163:**26–36. http://dx.doi.org/10.1016/j.cbpb.2012.05.006.

57. **Chang J, Klute MJ, Tower RJ, Mast FD, Dacks JB, Rachubinski RA.** 6 February 2015. An ancestral role in peroxisome assembly is retained by the divisional peroxin Pex11 in the yeast *Yarrowia lipolytica*. J Cell Sci http://dx.doi.org/10.1242/jcs.157743.